ResearchGate

See discussions, stats, and author profiles for this publication at: https://www.researchgate.net/publication/231389299

Thermogravimetric Analysis of Copper Oxide for Chemical-Looping Hydrogen Generation

ARTICLE *in* INDUSTRIAL & ENGINEERING CHEMISTRY RESEARCH · JULY 2008

Impact Factor: 2.59 · DOI: 10.1021/ie800174c

CITATIONS
25

READS
373

3 AUTHORS, INCLUDING:

Sang Done Kim
Korea Advanced Institute of Science and T…

365 PUBLICATIONS **5,555** CITATIONS

SEE PROFILE

Available from: Sang Done Kim
Retrieved on: 30 January 2016

Thermogravimetric Analysis of Copper Oxide for Chemical-Looping Hydrogen Generation

Sung Real Son, Kang Seok Go, and Sang Done Kim*

Department of Chemical and Biomolecular Engineering, Energy and Environment Research Center, Korea Advanced Institute of Science and Technology, Daejeon, 305-701, Korea

The chemical-looping hydrogen generation (CLH) system consists of reduction of metal oxide and water decomposition by oxidizing reduced metal oxide. In the present study, water decomposition by the reduction and oxidation of metal oxide (CuO) was conducted in a thermogravimetric analysis (TGA) system for the CLH process. The particles are reduced completely in an atmosphere of synthesis gas (H_2 + CO), and the fully reduced particles decompose water to produce 3.7 L of H_2 per kilogram of metal oxide. The particles prepared by the impregnation exhibits better reactivity than those by coprecipitation and the solid phase method, and the particles supported on Al_2O_3 exhibit better reactivity than those on SiO_2. Based on the TGA, the reduction and oxidation of CuO/Al_2O_3 prepared via impregnation are characterized by the kinetic equations from the solid-state reaction rate models. The phase-controlled-boundary model was successfully applied to predict the initial stages of reduction and oxidation of the metal oxide, and the activation energies for reduction and oxidation are determined to be 4.13−19.5 and −55.8 kJ/mol, respectively.

Introduction

Fossil fuels have many useful properties, but they are not renewable, they emit pollutants, and they have a depleting nature. Because hydrogen (H_2) is one of the most important alternative energy resources, H_2 generation from water is one of the most important long-term goals for future energy resources. Water splitting with the reduction and oxidation (redox) of a metal oxide, which is one of the H_2 production methods, does not produce harmful pollutants. In the reduction of a metal oxide for the water splitting process, however, a heat energy above 1500 K is needed, and solar energy is considered as a heat source with high construction and maintenance costs.[1] Furthermore, some metals could be melted and decomposed at high temperature, so additional technologies are needed to overcome this drawback.[2]

The steam methane reforming (SMR) process is widely used to produce H_2 on the industrial scale.[3] The SMR process consists of feed stock purification, steam reforming, a high-temperature shift reactor, a low-temperature shift reactor, H_2 separation, and CO_2 separation by methanation or pressure swing adsorption (PSA) processes. There are various H_2 production processes with methane, such as partial oxidation, thermal dissociation, reforming with CO_2, catalytic partial oxidation, plasma catalytic reforming, and direct cracking. However, most of conventional processes need H_2 purification and CO_2 separation processes.[4]

Chemical-looping hydrogen (CLH) generation, which originates from chemical-looping combustion (CLC),[5,6] is a type of water splitting process with a redox of metal oxide. The CLH system is composed of two reactors: an oxidation reactor, for water decomposition, and a reduction reactor, as shown in Figure 1. Reduction gas is introduced into the reduction reactor, where it reduces the metal oxide particles. The reduced metal oxide is circulated to the oxidation reactor, where it decomposes water to generate H_2 in this reaction. At complete conversion of the reduction gas, the exit gas stream from the reduction reactor contains only CO_2 and H_2O, and H_2 is emitted from the oxidation or water decomposition reactor with excess H_2O, so that pure H_2 and CO_2 can be obtained with H_2O condensation without a separation process.

The carbohydrate or synthesis gas fuel as a reduction gas is introduced into the reduction reactor, where it reacts with a metal oxide particle as

$$(2n+m)\mathrm{Me}_x\mathrm{O}_y + \mathrm{C}_n\mathrm{H}_{2m} \rightarrow (2n+m)\mathrm{Me}_x\mathrm{O}_{y-1} + n\mathrm{CO}_2 + m\mathrm{H}_2\mathrm{O} \quad (1)$$

$$\mathrm{Me}_x\mathrm{O}_y + \mathrm{H}_2 \rightarrow \mathrm{Me}_x\mathrm{O}_{y-1} + \mathrm{H}_2\mathrm{O} \quad (2)$$

$$\mathrm{Me}_x\mathrm{O}_y + \mathrm{CO} \rightarrow \mathrm{Me}_x\mathrm{O}_{y-1} + \mathrm{CO}_2 \quad (3)$$

The reduced metal oxide is then circulated to the water decomposition reactor, where it is oxidized with water, according to

$$\mathrm{Me}_x\mathrm{O}_{y-1} + \mathrm{H}_2\mathrm{O} \rightarrow \mathrm{Me}_x\mathrm{O}_y + \mathrm{H}_2 \quad (4)$$

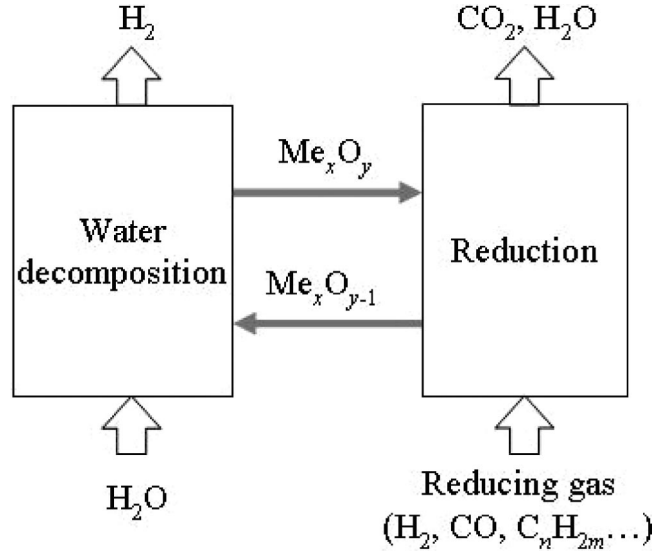

Figure 1. Conceptual diagram of chemical-looping hydrogen generation (CLH).

* Tel.: 82-42-869-3913, Fax: 82-42-869-3910, E-mail: kimsd@kaist.ac.kr

10.1021/ie800174c CCC: $40.75 © 2009 American Chemical Society
Published on Web 07/03/2008

The CLH system is simple one, because a water-gas shift reactor and CO_2 separation process are not needed. Moreover, only one type of particle is needed, whereas conventional SMR processes need more than four types of catalysts or absorbents. There is a novel concept to produce H_2 by chemical cycling, such as chemical-looping reformer (CLR),[7,8] where the fuel reactor acts as a reformer. The redox technology was proposed and evaluated for H_2 production;[9] however, it requires additional separation processes for H_2 and CO_2.

In this study, copper oxide (CuO) was selected for water decomposition and synthesis gas (H_2 + CO) was used for the lower-temperature reduction reaction. In most of the previous studies, ferrite or zinc-based materials were used for water splitting,[1,2,10–13] while CuO also has water splitting capacity at lower temperature. There are studies with copper ferrites for water decomposition,[14,15] but, so far, nobody has used pure CuO for water splitting, because it could melt at lower temperature before being reduced, but it could be applied in the CLH system, because the reducing gas makes the reaction occur at lower temperatures. Because the reduction temperature of other metal oxides, such as Fe_3O_4 and Mn_3O_4, is higher (>300 K) than that of CuO, the thermal efficiency would be higher. The water decomposition temperature of Fe_3O_4 is higher (>500 K) than that of CuO, so the overall heat consumption with CuO is much lower. Also, CuO allows complete fuel combustion to CO_2 and H_2O, and it is stable from carbon deposition.[16] CuO has an particle agglomeration problem in fluidized beds, whereas it can be used in a fixed bed and some modification of the preparation method to prohibit particle agglomeration.[17–19] The reactivity of each metal oxide was determined by thermogravimetric analysis, and the particles were prepared by the impregnation, coprecipitation, and solid phase methods, with alumina (Al_2O_3) and silica (SiO_2) as the supports. The mechanisms of the reduction and water decomposition reactions have been investigated by the kinetic equations used in the solid-state reaction models, and the activation energies and pre-exponential factors were determined.

Experimental Section

The metal oxide particles were prepared by the impregnation, coprecipitation, and solid phase methods. A copper nitrate ($Cu(NO_3)_2 \cdot 3H_2O$, Aldrich Chemical Co.) aqueous solution was mixed with γ-Al_2O_3 (Fluka) or SiO_2 xerogel (Aldrich) particles using the impregnation method. Water in this mixture was evaporated in a vacuum evaporator, and it was calcined at 923 K for 40 min. Particles 90−210 μm in size were prepared by sieving. An aqueous solution of copper nitrate with aluminum nitrate ($Al(NO_3)_3 \cdot 9H_2O$, Aldrich) was prepared for the coprecipitation, according to the method of a previous CLC study.[20] Solution of 2-propanol (Merck) was added and the mixture was dried at 373 K for 12 h, at 423 K for 24 h, and at 473 K for 5 h. It was calcined at 773 K for 2 h and then pasted again, dried at 353 K for 30 min, and calcined at 1573 K for 6 h. Also, the particle size was chosen to be 90−210 μm by sieving. For the solid phase method, CuO (Aldrich) was mixed with γ-Al_2O_3 in a ball mill for 18 h. The mixed powders were pasted by adding distilled water, dried at 383 K for 24 h, and calcined at 1173 K for 10 h. It then was crushed and sieved to prepare particle sizes in the range of 90−210 μm. For all the particles, the weight ratio of CuO to Al_2O_3 was 1.5.

Analysis using a scanning electron microscopy (SEM) system (Philips) showed the entire structure and microstructure of particles. Changes in the crystalline phase of the particles were analyzed using X-ray diffraction (XRD) (Rigaku D/MAX-III), with Cu Kα radiation, before and after each reaction. To determine the surface area of the particles, the Brunauer−Emmett−Teller (BET) method (NOVA-4200, v.7.10) with nitrogen adsorption was used.

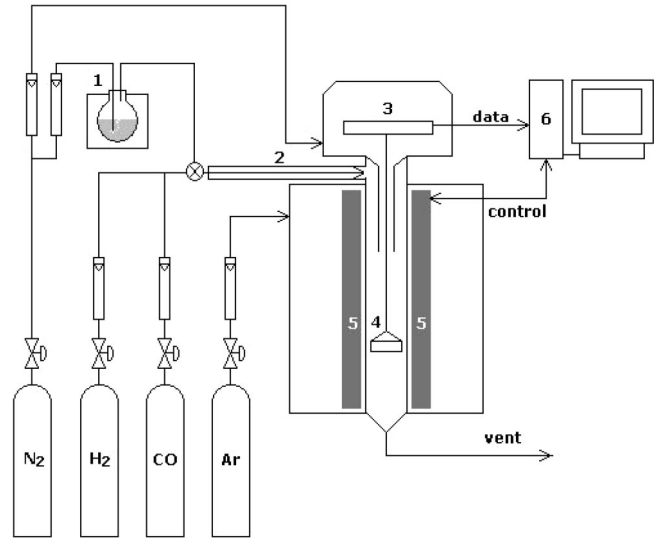

Figure 2. Schematic diagram of the thermogravimetric analysis (TGA) system for the reactivity test. Legend: (1) water reservoir and bubbler, (2) gas preheater, (3) electric balance, (4) sample basket, (5) heater, and (6) personal computer.

Reactivity of the reduction and water decomposition by CuO was determined in a thermogravimetric analysis (TGA) system (model Setaram 92). The prepared particles (10 mg) in a quartz basket were exposed to an atmosphere of 50% H_2 + 50% CO for reduction and 20% H_2O in N_2 for water decomposition. A schematic diagram of the TGA system is shown in Figure 2. The selected reaction temperature range was 623−1123 K for the reduction and 573−723 K for water decomposition.

Results and Discussions

Properties of Copper Oxide Particles. The chemical structures of the samples were characterized using powder XRD. Copper oxide particle by impregnation has only a CuO crystal phase, without phases related to Al_2O_3, compared to the particles formed via other preparation methods, as shown in Figure 3. It is observed that copper oxide was well-deposited on the surface of Al_2O_3. In the cases of the other two preparation methods, a copper aluminate ($CuAl_2O_4$) phase can be observed, and it may be formed with CuO and Al_2O_3 at higher temperatures.

The particle size of CuO was examined by SEM, as shown in Figure 4. Particles prepared via the impregnation method have smaller size, compared to those formed via the solid phase method and the coprecipitation method with the solution mixture. Preparation via the impregnation method is the metal oxide deposition method on the support particles (113−140 μm), and the other two methods are crushing the calcined loaves, so that smaller particles can be observed in the impregnation on the supports. However, particles prepared via any of the methods used are in the size range of 90−210 μm.

The surface area of the metal oxide, as determined by the N_2−BET method, is given in Table 1. Particles prepared via impregnation have much larger surface areas than those formed via the solid phase and coprecipitation methods. It is observed that the original pores of the γ-Al_2O_3 supports were retained during calcination, in the case of the impregnation with solution on the support particles, whereas pores were seldom generated

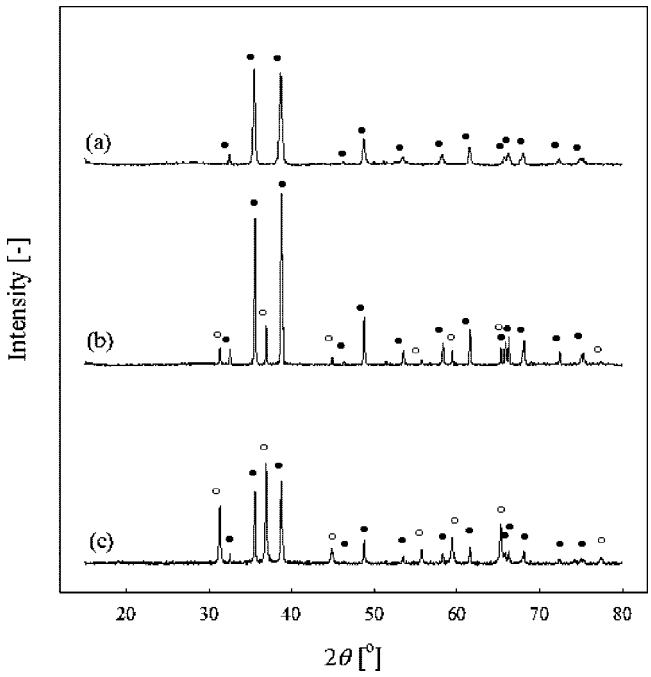

Figure 3. X-ray diffraction (XRD) spectra showing the crystalline phase of prepared copper oxide particles prepared by (a) the impregnation method, (b) the coprecipitation method, and (c) the solid phase method. Symbol legend: (●) CuO and (○) $CuAl_2O_4$.

by melting or phase changes at higher calcination temperature, in the case of the other two methods. The particles supported on SiO_2 exhibit somewhat higher surface area than that supported on Al_2O_3.

Reactivity of Copper Oxide Particles. Conversions of the reduction and water decomposition of metal oxide particles can be defined as follows:

$$\text{Reduction:} \qquad X = \frac{m_{ox} - m}{m_{ox} - m_{red}} \tag{5}$$

$$\text{Water Decomposition:} \qquad X = \frac{m - m_{red}}{m_{ox} - m_{red}} \tag{6}$$

where m, m_{red} and m_{ox} are, respectively, the weight of sample, the weight of sample after being fully reduced, and the weight of sample after being fully oxidized. The value of m_{red} is determined to that of metallic copper, because they can be reduced under the strong reducing conditions.

The reduction conversions of CuO/Al_2O_3 at 923 K, using the different preparation methods, are shown in Figure 5. The reactivity of CuO/Al_2O_3 particles prepared via impregnation is the best among the prepared methods for the reduction reactions. The reduction conversion of the particles prepared via the coprecipitation method is >0.9 within 20 s, and the conversion by the solid phase method also exhibits values that are lower than those obtained using the other two methods. As can be observed, there was no carbon deposition on the metal oxides during the reaction up to 40 s. The higher reactivity of the particle may be attributed to the initial crystal phase and higher surface area of the particle. The lower reactivity may be caused by lower oxygen emission capacity of crystalline $CuAl_2O_4$ than that of CuO.

The conversions of reduction and water decomposition reactions of CuO on the different supports are shown in Figures 6 and 7, respectively. The results are compared at 923 K for reduction and at 623 K for water decomposition. As can be

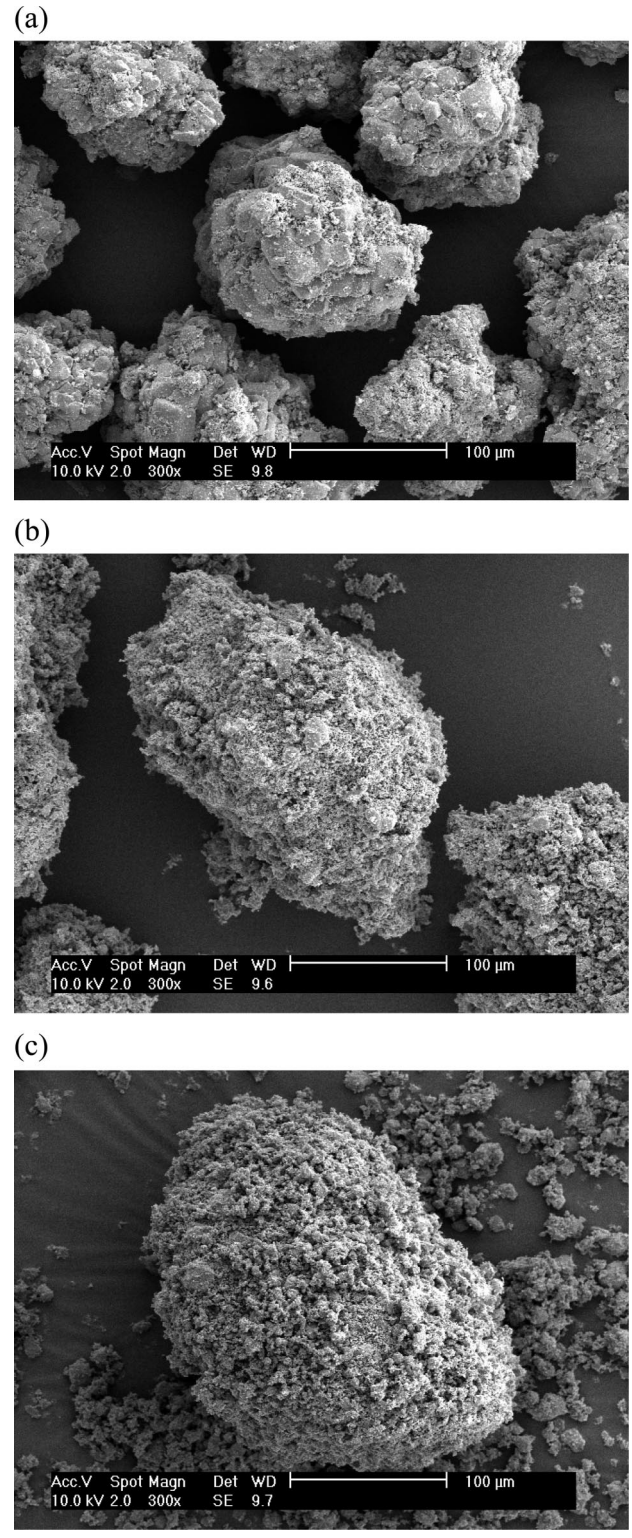

Figure 4. SEM images of prepared copper oxide particles prepared by (a) the impregnation method, (b) the coprecipitation method, and (c) the solid phase method.

observed, the reactivity of CuO supported on Al_2O_3 is faster for the both reactions than that on SiO_2. The specific crystalline phases of CuO/Al_2O_3 and CuO/SiO_2 are similar to CuO, and CuO/SiO_2 exhibits greater surface area than CuO/Al_2O_3, whereas SiO_2 gel powder has structural weaknesses at higher temperature, compared to Al_2O_3, and the calcination temperature is lower than the reaction temperature, because of the exothermic reaction, so it is predicted that the physical and chemical composition of CuO/SiO_2 may be changed in the reduction

Table 1. Main Crystalline Phase and Surface Area of the Metal Oxide Particles

specimen	preparation method	main crystalline phase(s)	surface area (m^2/g)
CuO/Al_2O_3	impregnation	CuO	84.34
CuO/Al_2O_3	coprecipitation	CuO, $CuAl_2O_4$	1.60
CuO/Al_2O_3	solid phase method	CuO, $CuAl_2O_4$	4.92
CuO/SiO_2	impregnation	CuO	145.68

reaction. Based on these results, CuO/Al_2O_3 particles prepared using the impregnation method was selected for the kinetic study.

The reduction and oxidation conversions of CuO/Al_2O_3 prepared via the impregnation method at different reaction

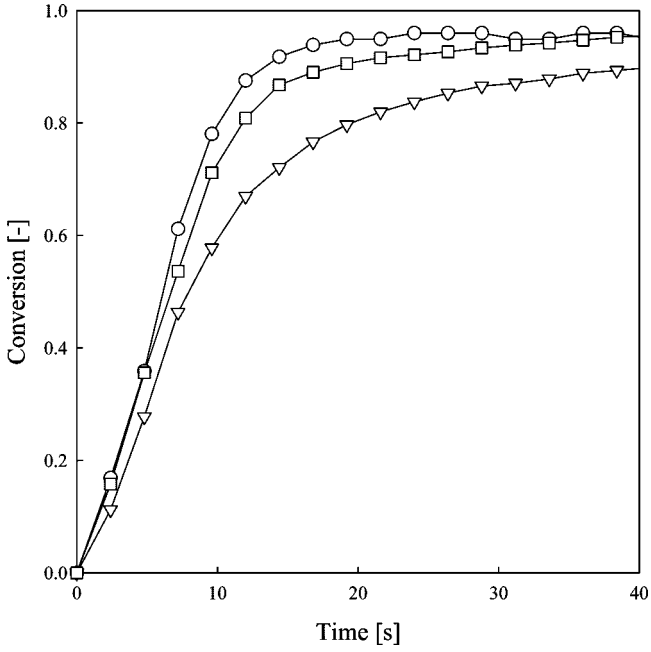

Figure 5. Reduction reactivity of CuO/Al_2O_3 by different preparation methods at 923 K: (○) impregnation method, (□) coprecipitation method, and (▽) solid phase method.

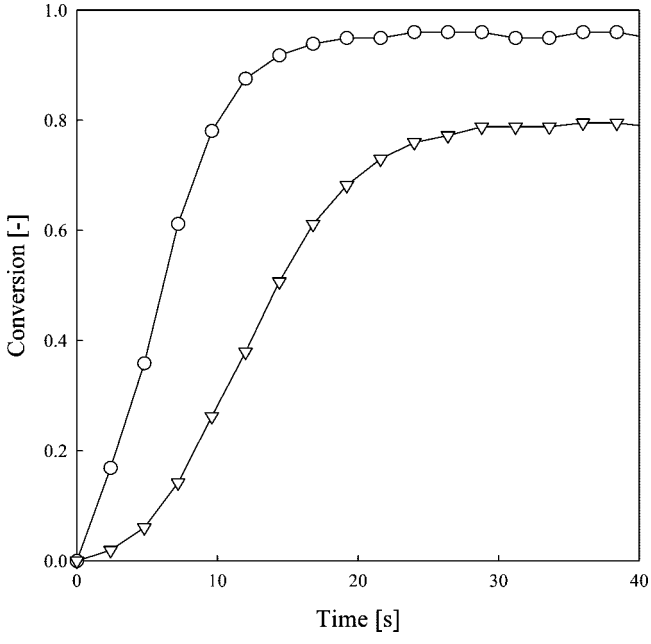

Figure 6. Reduction reactivity of CuO at 923 K on different supports: (○) Al_2O_3 support and (▽) SiO_2 support.

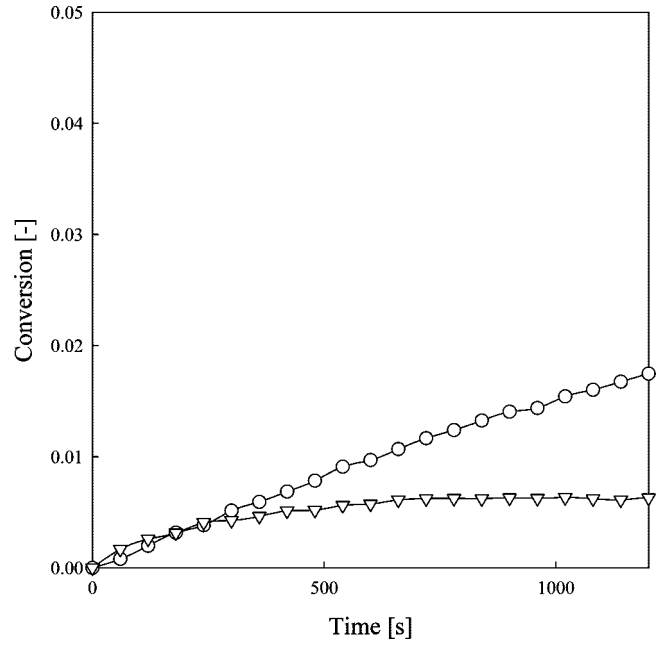

Figure 7. Oxidation reactivity of copper on different supports by water decomposition at 623 K: (○) Al_2O_3 support and (▽) SiO_2 support.

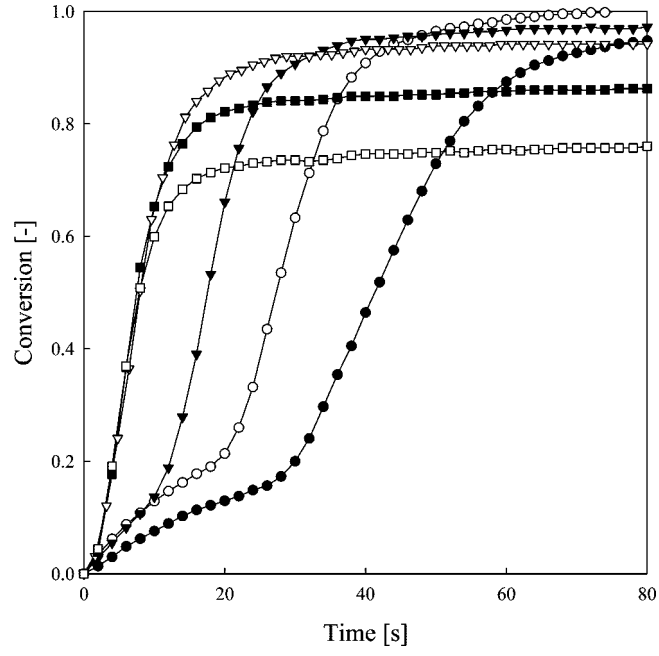

Figure 8. Reduction conversion of CuO/Al_2O_3 with time at different reaction temperatures: (●) 623, (○) 723, (▼) 823, (▽) 923, (■) 1023, and (□) 1123 K.

temperatures are shown in Figures 8 and 9, respectively. The reactivity increases as the reaction temperature increases for the reduction, and the conversion is slow in the early stage and faster in the later stage. The division of stages may be caused by phase change steps from CuO to Cu_2O and from Cu_2O to metallic copper. This division disappears with increasing temperature as the conversion is increased. At higher temperatures (>923 K), the final conversion is lower with higher reaction temperatures. It may be caused by the formation of crystalline $CuAl_2O_4$ or by the side reactions, such as a reaction of H_2 and CO by themselves, activated at higher temperature. Therefore, the optimum reduction temperature would be 923 K. For the water decomposition, the optimum temperature is exhibited at 623 K. At lower temperatures (<623 K), water

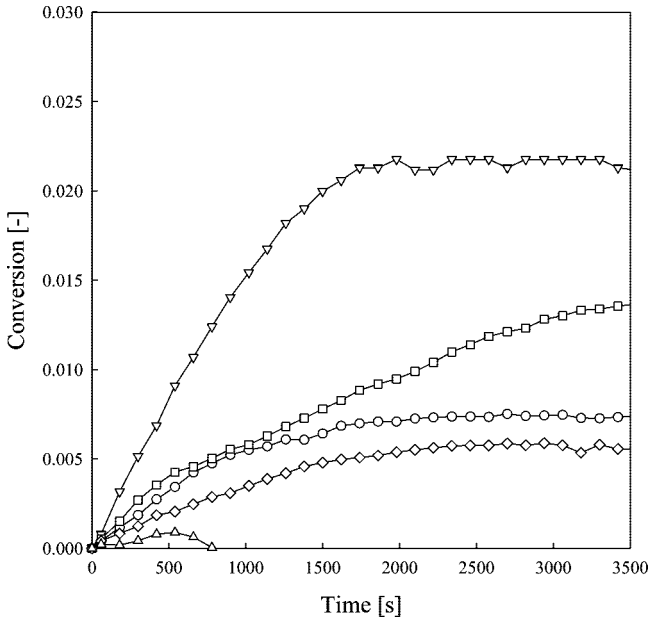

Figure 9. Oxidation conversion of Cu/Al_2O_3 by water decomposition with time at different reaction temperatures: (○) 573, (▽) 623, (□) 673, (◇) 723, and (△) 773 K.

splitting activates with increased reaction temperature, whereas free O atoms can be produced via the thermal reduction of a metal oxide at higher temperature. The free O atoms by thermal reduction may bond together as an oxygen molecule, or they may react with H_2 from the water split, so weight of the metal oxide may decrease and the reactivity also decreases at higher temperatures, as calculated previously.[21] From the conversion data, the calculated hydrogen production is 3.7 L of H_2 per kilogram of CuO/Al_2O_3, under the optimum reaction conditions.

Reaction Kinetics of Copper Oxide Particles. Hancock and Sharp[22] have described a convenient method of comparing the kinetics of isothermal solid-state reactions based on an equation that describes the nucleation and growth processes. The experimental data can be expressed as the following equations:

$$X = 1 - \exp(-at^b) \tag{7}$$

$$\ln(-\ln(1 - X)) = \ln a + b \ln t \tag{8}$$

where a is a constant that is partially dependent on the nucleation frequency and rate of grain growth, and b is a constant that varies with the geometry of the system. The constants a and b are determined from the Hancock and Sharp plot by $-\ln(\ln(1 - X))$ vs $\ln t$. The slopes of such plots can be used as a diagnostic tool to determine the reaction mechanism. Hancock and Sharp treated nine kinetic equations, which could arbitrarily be separated into three groups, namely, diffusion-controlled reactions, phase-boundary-controlled and first-order reactions, and the reactions that obey the Avrami−Erofe'ev phase change equations. The functions $D_1(X)$ through $D_4(X)$ represent some of the important diffusion equations. $F_1(X)$ is the function for first-order reactions, and $R_2(X)$ and $R_3(X)$ are the equations for phase-boundary-controlled reactions for a cylinder or a circular disk and a sphere, respectively. $A_2(X)$ and $A_3(X)$ are the Avrami−Erofe'ev equations for $b = 2.0$ and 3.0, respectively. The selected rate equations of the solid-state reaction are shown in Table 2. Details of the equations and reaction mechanism can be found elsewhere.[23,24]

The Hancock and Sharp plots for the reduction reaction of CuO/Al_2O_3 prepared via impregnation are shown in Figure 10, from which the b parameter values were determined as listed in Table 3. The values of b are in the range of 0.8−2.0 for the initial stage of reduction at the selected temperature from Figure

Table 2. Solid-State Reaction Rate Equations[a]

function	equation	equation number	value of b
$D_1(X)$	$X^2 = kt$	(9)	0.62
$D_2(X)$	$(1 - X)\ln(1 - X) + X = kt$	(10)	0.57
$D_3(X)$	$[1 - (1 - X)^{1/3}]^2 = kt$	(11)	0.54
$D_4(X)$	$1 - 2X/3 - (1 - X)^{2/3} = kt$	(12)	0.57
$F_1(X)$	$-\ln(1 - X) = kt$	(13)	1.00
$R_2(X)$	$1 - (1 - X)^{1/2} = kt$	(14)	1.11
$R_3(X)$	$1 - (1 - X)^{1/3} = kt$	(15)	1.07
zero order	$X = kt$	(16)	1.24
$A_2(X)$	$[-\ln(1 - X)]^{1/2} = kt$	(17)	2.00
$A_3(X)$	$[-\ln(1 - X)]^{1/3} = kt$	(18)	3.00

[a] Data taken from ref 22.

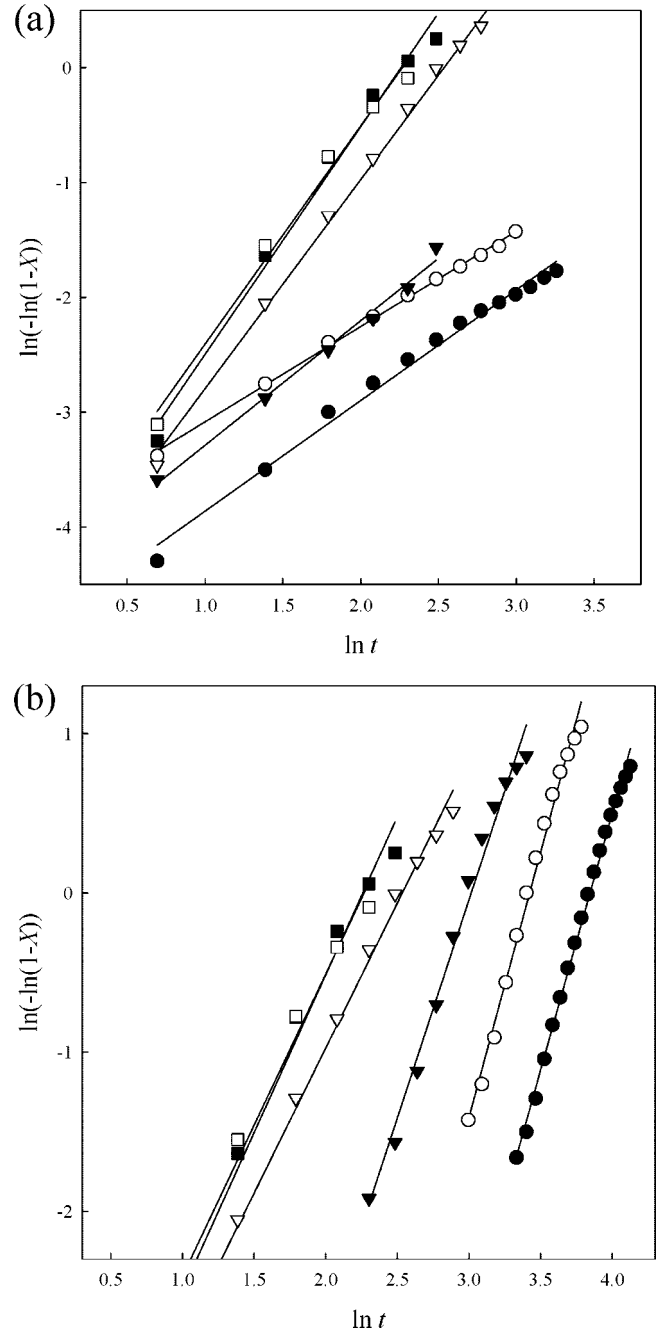

Figure 10. Plots of the Hancock and Sharp procedure for the reduction of CuO/Al_2O_3: (a) CuO → Cu_2O at <823 K; (b) Cu_2O → Cu at <823K. Legend: (●) 623 K, (○) 723 K, (▼) 823 K; (▽) 923 K, (■) 1023 K, and (□) 1123 K.

Table 3. Parameter *b* Values in the Reduction of CuO/Al_2O_3

T (K)	Phase Change	b	correlation coefficient, r^2
623	$CuO \rightarrow Cu_2O$	0.96	0.990
623	$Cu_2O \rightarrow Cu$	3.22	0.996
723	$CuO \rightarrow Cu_2O$	0.80	0.998
723	$Cu_2O \rightarrow Cu$	3.33	0.990
823	$CuO \rightarrow Cu_2O$	1.09	0.991
823	$Cu_2O \rightarrow Cu$	2.74	0.988
923	$CuO \rightarrow Cu$	1.82	0.996
1023	$CuO \rightarrow Cu$	1.98	0.988
1123	$CuO \rightarrow Cu$	1.90	0.988

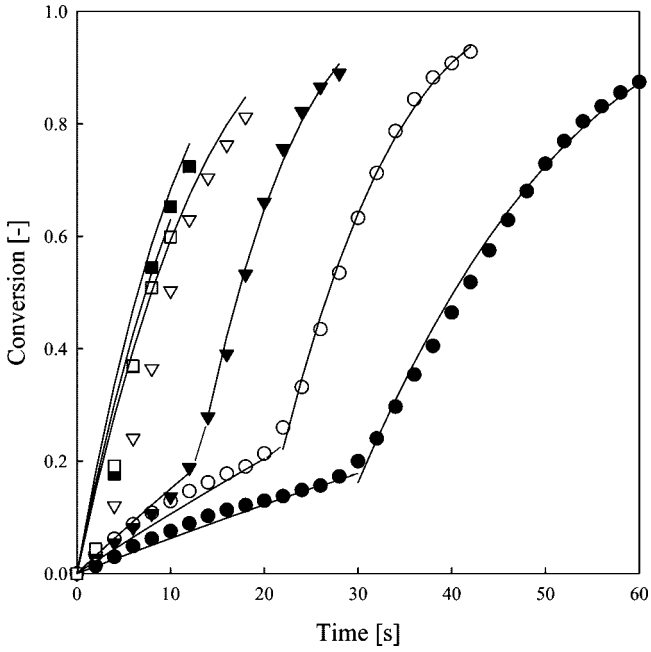

Figure 11. Comparison between the experimental data and the phase-boundary-controlled model for the reduction of CuO/Al_2O_3: (●) 623, (○) 723, (▼) 823, (▽) 923, (■) 1023, and (□) 1123 K (the solid line represents the phase-boundary-controlled model).

10a; thus, the phase-boundary-controlled reaction rate model ($R_3(X)$) was selected to analyze the experimental data. Moreover, the latter stages for changing the phases from Cu_2O to copper have b values in the range of 2.7−3.4 (from Figure 10b), so that the Avrami−Erofe'ev phase change model was also applied to the kinetic study. Using the equations in Table 2, the reaction constant k was determined by the solid-state reaction rate models. Between the models, it has been observed that the phase-boundary-controlled reaction model is the best representation of the reduction of CuO/Al_2O_3, with a correlation coefficient of $r^2 > 0.98$. The Avrami−Erofe'ev phase change model represents the reaction stages well from Cu_2O to copper at temperature below 823 K, but it does not produce reasonable accuracy for the other stages. The agreement between the experimental data of the reduction of CuO/Al_2O_3 and the predicted data from the phase-boundary-controlled reaction model is good, as shown in Figure 11.

The activation energy and pre-exponential factor of each step of reduction were determined from the Arrhenius plot. According to the reaction temperature, the activation energies and pre-exponential factors were determined for the early and later stages of the reduction at temperatures <823 K and the entire reduction was observed to occur at >923 K.

$$k = 9.26 \times 10^{-2} \exp\left(\frac{-19.5\ \text{kJ/mol}}{RT}\right) \quad (\text{for } CuO \rightarrow Cu_2O \text{ at } < 823\ \text{K}) \quad (19)$$

$$k = 3.83 \times 10^{-1} \exp\left(\frac{-16.7\ \text{kJ/mol}}{RT}\right) \quad (\text{for } Cu_2O \rightarrow Cu \text{ at } < 823\ \text{K}) \quad (20)$$

$$k = 4.65 \times 10^{-2} \exp\left(\frac{-4.13\ \text{kJ/mol}}{RT}\right) \quad (\text{for } CuO \rightarrow Cu \text{ at } > 923\ \text{K}) \quad (21)$$

For the oxidation of Cu/Al_2O_3 by water decomposition, the plots of Hancock and Sharp's procedure are shown in Figure 12, from which the parameter b values were determined, as shown in Table 4. The b values are determined to be in the range of 0.78−0.99, which lies in the category between the diffusion-controlled reaction and the phase-boundary-controlled reaction. To determine the k values, the diffusion-controlled reaction and phase-boundary-controlled reaction models were used, and it was determined that the phase-boundary-controlled reaction model fits better than the diffusion-controlled reaction model with correlation coefficients of >0.97. The agreement between the experimental data and the phase-boundary-controlled reaction model is shown in Figure 13 for the oxidation of Cu/Al_2O_3 by water decomposition.

The activation energy and pre-exponential factor of oxidation by water decomposition was determined from the Arrhenius plot. The reactivity decreases with increasing reaction temperature above 673 K, so that the activation energy has a negative value in the oxidation of Cu/Al_2O_3 by water decomposition.

$$k = 8.93 \times 10^{-11} \exp\left(\frac{+55.8\ \text{kJ/mol}}{RT}\right) \quad (\text{at} < 673\ \text{K}) \quad (22)$$

Conclusion

For the chemical-looping hydrogen (CLH) system, CuO particles were prepared by the impregnation, coprecipitation, and solid phase methods. The reactivity of CuO/Al_2O_3 and CuO/SiO_2 were determined in a thermogravimetric analysis (TGA) system with alternating reduction (50% H_2 + 50% CO) and

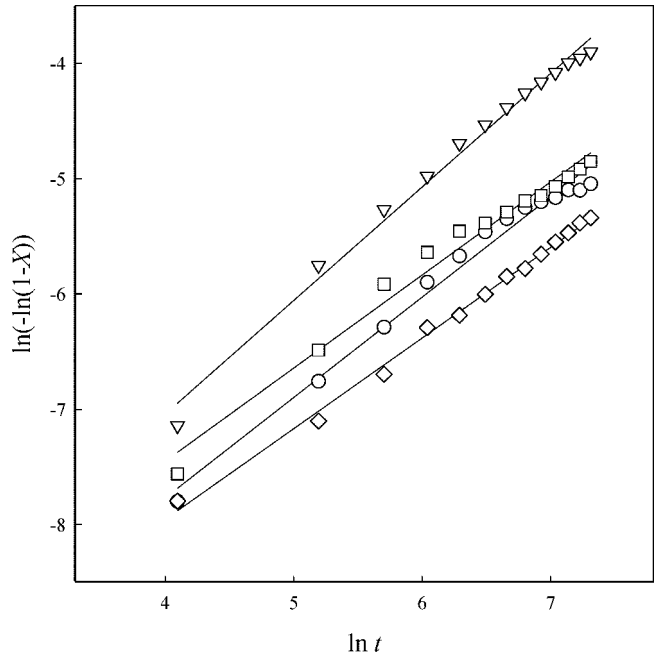

Figure 12. Plots of Hancock and Sharp's procedure for water decomposition of Cu/Al_2O_3: (○) 573 K, (▽) 623 K, (□) 673 K, and (◇) 723 K.

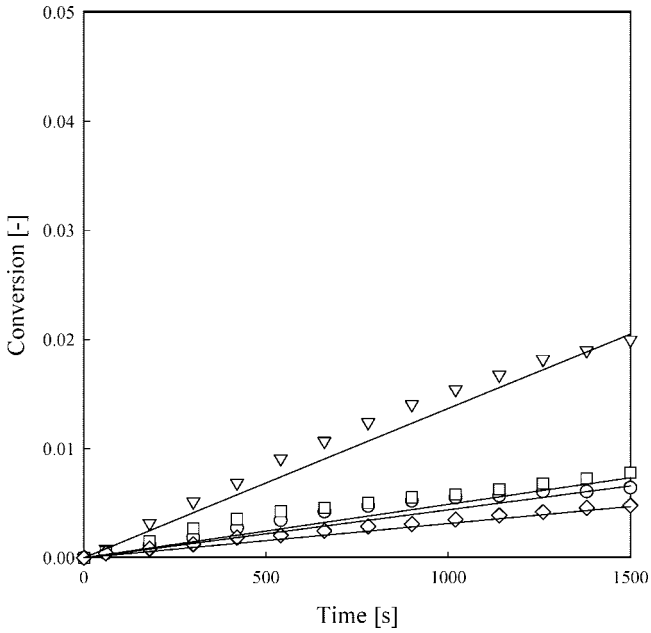

Figure 13. Comparison between the experimental data and the phase-boundary-controlled model for water decomposition of Cu/Al_2O_3: (○) 573 K, (▽) 623 K, (□) 673 K, and (◇) 723 K (the solid line represents the phase-boundary-controlled model).

Table 4. Parameter *b* Values in the Oxidation of Cu/Al_2O_3 by Water Decomposition

temperature, T (K)	b	correlation coefficient, r^2
573	0.87	0.985
623	0.98	0.990
673	0.81	0.980
723	0.79	0.996

oxidation (20% H_2O in N_2) reactions. The particles prepared by the impregnation method exhibits better reactivity than those by the coprecipitation and solid phase methods, and the particles supported on Al_2O_3 exhibits better reactivity than those on SiO_2. The reduction reactivity of CuO increases as the reaction temperature increases, and the conversion is slow in the early stage and faster in the later stage. The optimum reduction temperature is determined to be 923 K, and the optimum water decomposition temperature is 623 K. The reduction and oxidation kinetic data of CuO/Al_2O_3 prepared via impregnation are characterized by the kinetic solid-state reaction rate models. The phase-controlled-boundary model represents the initial stages of reduction and oxidation well, and the activation energies for the reduction and oxidation are determined to be 4.13−19.5 kJ/mol and −55.8 kJ/mol, respectively.

Acknowledgment

This work was supported by Ministry of Commerce, Industry and Energy (MOCIE) through Electric Power Industry Technology Evaluation and Planning Center (ETEP) and the Brain Korea 21 Project from the Ministry of Education.

Nomenclature

a, b = constants determined from the Hancock and Sharp plot
k = reaction rate constant in the solid-state reaction rate model (s^{-1})
m = actual sample mass of metal oxide (g)
m_{ox} = mass of metal oxide sample when fully oxidized (g)
m_{red} = mass of metal oxide sample when fully reduced (g)
R = gas constant (J kg^{-1} mol^{-1} K^{-1})
r^2 = correlation coefficient
t = time (s)
X = conversion of metal oxide (from eqs 5 and 6)

Literature Cited

(1) Kodama, T.; Kondoh, Y.; Yamamoto, R.; Andou, H.; Satou, N. Thermochemical Hydrogen Production by a Redox System of ZrO_2-Supported Co(II)-Ferrite. *Sol. Energy* **2005**, *78*, 623–631.

(2) Wegner, K.; Ly, H. C.; Weiss, R. J.; Pratsinis, S. E.; Steinfeld, A. In Situ Formation and Hydrolysis of Zn Nonoparticles for H_2 Production by the 2-Step ZnO/Zn Water-Splitting Thermochemical Cycle. *Int. J. Hydrogen Energy* **2006**, *31*, 55–61.

(3) Wang, Y. N.; Rodrigues, A. E. Hydrogen Production from Steam Methane Reforming Coupled with in Situ CO_2 Capture: Conceptual Parametric Study. *Fuel* **2005**, *84*, 1778–1789.

(4) Jin, G. T.; Ryu, H.-J.; Jo, S.-H.; Lee, S.-Y.; Son, S. R.; Kim, S. D. Hydrogen Production in Fluidized Bed by Chemical-Looping Cycle. *Korean J. Chem. Eng.* **2007**, *24*, 542–546.

(5) Richter, H. J.; Knoche, K. F. Reversibility of Combustion Process. In *ACS Symposium Series*; American Chemical Society: Washington, DC, 1983; pp 71−85.

(6) Ishida, M.; Zheng, D.; Akehata, T. Evaluation of a Chemical-Looping Combustion Power-Generation System by Graphic Exergy Analysis. *Energy* **1987**, *12*, 147–154.

(7) Zafar, Q.; Mattisson, T.; Gevert, B. Integrated Hydrogen and Power Production with CO_2 Capture Using Chemical-Looping Reforming—Redox Reactivity of Particles of CuO, Mn_2O_3, NiO, and Fe_2O_3 Using SiO_2 as a Support. *Ind. Eng. Chem. Res.* **2005**, *44*, 3485–3496.

(8) Rydén, M.; Lyngfelt, A.; Mattisson, T. Synthesis Gas Generation by Chemical-Looping Reforming in a Continuously Operating Laboratory Reactor. *Fuel* **2006**, *85*, 1631–1641.

(9) Sime, R.; Kuehni, J.; D'Souza, L.; Elizondo, E.; Biollaz, S. The Redox Process for Producing Hydrogen from Woody Biomass. *Int. J. Hydrogen Energy* **2003**, *28*, 491–498.

(10) Ehrensberger, K.; Frei, A.; Kuhn, P.; Oswald, H. R.; Hug, P. Comparative Experimental Investigations of the Water-Splitting Reaction with Iron Oxide $Fe_{1-y}O$ and Iron Manganese Oxides $(Fe_{1-x}Mn_x)_{1-y}O$. *Solid State Ionics* **1995**, *78*, 151–160.

(11) Urasaki, K.; Tanimoto, N.; Hayashi, T.; Sekine, Y.; Kikuchi, E.; Matsukata, M. Hydrogen Production via Steam-Iron Reaction Using Iron Oxide Modified with Very Small Amounts of Palladium and Zirconia. *Appl. Catal., A* **2005**, *288*, 143–148.

(12) Alvani, C.; Ennas, G.; La Barbera, A.; Marongiu, G.; Padella, F.; Varsano, F. Synthesis and Characterization of Nanocrystalline $MnFe_2O_4$: Advances in Thermochemical Water Splitting. *Int. J. Hydrogen Energy* **2005**, *30*, 1407–1411.

(13) Tamaura, Y.; Kojima, N.; Hasegawa, N.; Inoue, M.; Uehara, R.; Gokon, N.; Kaneko, H. Stoichiometric Studies of H_2 Generation Reaction for $H_2O/Zn/Fe_3O_4$ System. *Int. J. Hydrogen Energy* **2001**, *26*, 917–922.

(14) Kaneko, H.; Yokoyama, T.; Fuse, A.; Ishihara, H.; Hasegawa, N.; Tamaura, Y. Synthesis of New Ferrite, Al-Cu Ferrite, and Its Oxygen Deficiency for Solar H_2 Generation from H_2O. *Int. J. Hydrogen Energy* **2006**, *31*, 2256–2265.

(15) Peña, J. A.; Lorente, E.; Romero, E.; Herguido, J. Kinetic Study of the Redox Process for Storing Hydrogen Reduction Stage. *Catal. Today* **2006**, *116*, 439–444.

(16) Adánez, J.; García-Labiano, F.; de Diego, L. F.; Gayán, P.; Celaya, J.; Abad, A. Nickel−Copper Oxygen Carriers to Reach Zero CO and H_2 Emissions in Chemical-Looping Combustion. *Ind. Eng. Chem. Res.* **2006**, *45*, 2617–2625.

(17) de Diego, L. F.; Gayán, P.; García-Labiano, F.; Celaya, J.; Abad, A.; Adánez, J. Impregnated CuO/Al_2O_3 Oxygen Carriers for Chemical-Looping Combustion: Avoiding Fluidized Bed Agglomeration. *Energy Fuels* **2005**, *19*, 1850–1856.

(18) de Diego, L. F.; García-Labiano, F.; Adánez, J.; Gayán, P.; Abad, A.; Corbella, B. M.; Palacios, J. M. Development of Cu-Based Oxygen Carriers for Chemical-Looping Combustion. *Fuel* **2004**, *83*, 1749–1757.

(19) Corbella, B. M.; de Diego, L. F.; García-Labiano, F.; Adánez, J.; Palacios, J. M. Characterization and Performance in a Multicycle Test in a Fixed-Bed Reactor of Silica-Supported Copper Oxide as Oxygen Carrier for Chemical-Looping Combustion of Methane. *Energy Fuels* **2006**, *20*, 148–154.

(20) Ishida, M.; Yamamoto, M.; Ohba, T. Experimental Results of Chemical-Looping Combustion with $NiO/NiAl_2O_4$ Particle Circulation at 1200 °C. *Energy Conserv. Manage.* **2002**, *43*, 1469–1478.

(21) Aoki, A.; Ohtake, H.; Shimizu, T.; Kitayama, Y.; Kodama, T. Reactive Metal-Oxide Redox System for a Two-Step Thermochemical Conversion of Coal and Water to CO and H_2. *Energy* **2000**, *25*, 201–218.

(22) Hancock, J. D.; Sharp, J. H. Method of Comparing Solid-State Kinetic Data and Its Application to the Decomposition of Kaolinite, Brucite, and $BaCO_3$. *J. Am. Ceram. Soc.* **1972**, *55*, 74–77.

(23) Piotrowski, K.; Mondal, K.; Lorethova, H.; Stonawski, L.; Szymañski, T.; Wiltowski, T. Effect of Gas Composition on the Kinetics of Iron Oxide Reduction in a Hydrogen Production Process. *Int. J. Hydrogen Energy* **2005**, *30*, 1543–1554.

(24) Piotrowski, K.; Mondal, K.; Wiltowski, T.; Dydo, P.; Rizeg, G. Topochemical Approach of Kinetics of the Reduction of Hematite to Wüstite. *Chem. Eng. J.* **2007**, *131*, 73–82.

Received for review January 31, 2008
Revised manuscript received March 21, 2008
Accepted April 1, 2008

IE800174C